
Article:
Robinson, A. P. L. and Pasley, J. orcid.org/0000-0001-5832-8285 (2018) Potential for the Vishniac instability in ionizing shock waves propagating into cold gases. Physics of Plasmas. 052701. ISSN 1089-7674

https://doi.org/10.1063/1.5025032

This manuscript was accepted by Phys. Plasmas. Click here to see the version of record.

Potential for the Vishniac instability in Ionizing Shock Waves Propagating into Cold Gases

A.P.L.Robinson[1] and J.Pasley[2]
[1)] *Central Laser Facility, STFC Rutherford-Appleton Laboratory, Didcot, OX11 0QX, United Kingdom*
[2)] *York Plasma Institute, Department of Physics, University of York, York YO10 5DD, United Kingdom*

(Dated: 5 April 2018)

The Vishniac instability was posited as an instability that could affect supernova remnants in their late stage of evolution when subject to strong radiative cooling, which can drive the effective ratio of specific heats below 1.3. The potential importance of this instability to these astrophysical object has motivated a number of laser-driven laboratory studies. However the Vishniac instability is essentially a dynamical instability that should operate independently of whatever physical processes happen to reduce the ratio of specific heats. In this paper we examine the possibility that ionization and molecular dissociation processes can achieve this, and we show that this is possible for a certain range of shock wave Mach numbers for ionizing/dissociating shock waves propagating into cold atomic and molecular gases.

I. INTRODUCTION

The stability of shock waves is a matter of fundamental importance in hydrodynamics and plasma physics[1], because of the wide-ranging consequences that it entails. The stability of shock waves has implications for subjects that range from the structure of supernova remnants (SNRs) through to the prospects of inertial confinement fusion. There appears to be general agreement that planar and divergent shock waves propagating in an ideal gas are stable[2], although convergent (imploding) shocks are unstable[3]. Real fluids always deviate from ideal fluids in certain areas of parameter space, or are subject to more physical processes than are embodied by the equations of Eulerian hydrodynamics. Fluids that possess non-ideal equations of state can be susceptible to the D'yakov-Kontorovich instability[4,5], for example.

In the case of radiative blast waves[6], the blast wave front is theoretically susceptible to the Vishniac instability[7–9]. The Vishniac instability has attracted considerable attention because of its potential to explain complex structures in SNRs[10] and in other astrophysical phenomena[11–13]. It has been pointed out by certain authors that the role of this instability in these astrophysical objects is not a fully resolved matter[10]. Nonetheless this interest has spurred a number of researchers to carry out experiments using high-powered lasers to investigate this instability[14–19].

There are a number of questions about the interpretation of laser-driven blast wave experiments aimed at either studying the Vishniac instability or other exotic hydrodynamic instabilities. The central theme of these questions is whether the influence of other physical processes can be sufficiently excluded as to ensure that only the instability in question can be studied in isolation. For example, it was noted by Symes[17] that radiative blast waves launched in high-Z gases (e.g. Xe) may not exhibit sufficiently strong compression for the Vishniac instability to occur, due to the complex structure of the shock fronts in the radiative regime. In another case, Nilson[20] argued that a shock front instability observed in a blast wave launched in He was due to the D'yakov-Kontorovich instability, and implicitly excluded the Vishniac instability as the radiative losses would be negligible. However, as Symes also noted, the Vishniac instability (and related instabilities) do not specifically depend on radiative cooling, rather they depend on the fluid being more compressible than an ideal gas. For the case of a fluid with a polytropic equation of state this should occur for $\gamma < 1.3$ (where γ is the ratio of specific heat capacities).

In this paper we pick up on this aforementioned remark by Symes, and we examine the potential for the Vishniac instability (and related instabilities) to occur when shocks propagate into cold gases. This builds on the ionization mechanism for lowering γ that has been noted in astrophysical studies[21]. We argue that this is possible in the case where the shock is partially ionizing or dissociating (in the case of propagation into molecular gases), as in this case the ionization/dissocation processes become a source of energy loss that can cause γ to fall well below 5/3. We have structured the paper as follows: In Section II we start by showing the occurrence of low γ in the case of a 'toy' model in which the fluid consists only of atomic hydrogen. In Sections III and IV we then look at shock wave propagation in helium and diatomic hydrogen gas and show that a post-shock γ below 1.3 can be achieved in both cases. In Section V we present the results of numerical simulations that show the development of a Vishniac-like instability when we use the EOS for molecular hydrogen. We then state our conclusions in Section VI.

II. HYDROGEN IONIZATION

We start by looking at the simplest thermodynamic model for an ionizing fluid : dilute atomic hydrogen. In this model the formation of the H_2 molecule is neglected,

and the only species that are considered are H,H^+ and e^-. For a given temperature and mass density, the densities of these species can be determined from the Saha equation:

$$\frac{n_{H^+}n_e}{n_H} = \left(\frac{2\pi m_e k_B T}{h^2}\right)^{3/2} e^{-\epsilon_i/k_B T}. \quad (1)$$

In Eq. 1, ϵ_i is the ionization energy, and all other symbols have their usual meaning. Given that $n_e = n_{H^+}$, if we introduce the 'total' atomic density, $n_0 = \rho/m_p = n_H + n_{H^+}$, and define the ionization fraction, $f = n_{H^+}/n_0$, then we can re-write this as,

$$\frac{f^2}{1-f} = \frac{1}{n_0}\left(\frac{2\pi m_e k_B T}{h^2}\right)^{3/2} e^{-\epsilon_i/k_B T} = K, \quad (2)$$

which is a quadratic equation. The solution being,

$$f = \frac{1}{2}\left(\sqrt{K^2+4K} - K\right). \quad (3)$$

The equation of state for this model can then be specified by,

$$P = n_0 k_B T(1+f), \quad (4)$$

and

$$U = \frac{3}{2}n_0 k_B T(1+f) + \epsilon_i n_0 f \quad (5)$$

We can now calculate γ using these relations (see Appendix). In fig.1 we plot γ against temperature for this model for the case of $n_0 = 2.5\times10^{24}\mathrm{m}^{-3}$. At low and high temperatures we see that $\gamma \approx 5/3$, which is expected as this model corresponds to an ideal gas in both the fully neutral and fully ionized limits. However there is a temperature range (1-2 eV at this density) over which the fluid is a partially ionized plasma, and here the ratio of specific heats falls substantially below 5/3. Fig. 1 clearly shows that the ratio of specific heats falls below 1.3. This shows that, in principle, ionization processes can produce a partially ionized plasma with a ratio of specific heats below 1.3.

It is also important, at this point, to note that neglecting the molecular state of hydrogen is not the only simplification that this model makes. This model also neglects the excited states of neutral hydrogen, for example. Although this suggests that ionizing shock wave propagation into cold gases can be subject to the Vishniac instability, we need to show that: (a) this occurs for more realistic equations of state, and (b) that there exist post-shock states with γ <1.3. Here we demonstrated that there exist some thermodynamic states for which γ <1.3, but these are not necessarily post-shock states. We will now proceed to demonstrate that post-shock states satisfy this in the following sections.

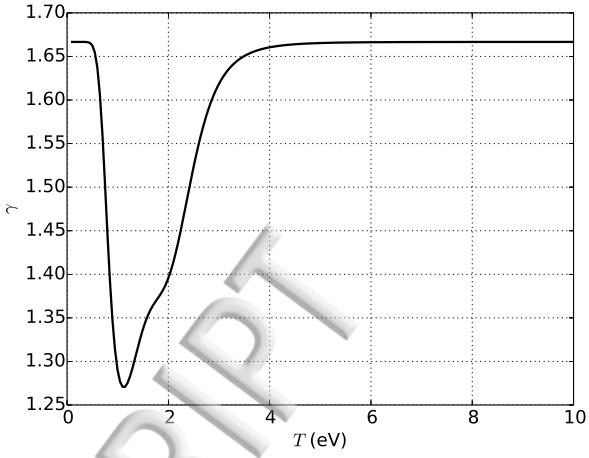

FIG. 1. Plot of the ratio of specific heats,γ versus temperature (in eV) for the atomic hydrogen model at $n_0 = 2.5\times10^{24}\mathrm{m}^{-3}$.

III. SHOCK PROPAGATION IN HELIUM

In the preceding section we considered the equation of state for purely atomic hydrogen, which is not an especially realistic equation of state given that it neglects the molecular form of hydrogen. The equation of state for helium can be obtained in a similar fashion. As helium does not have a molecular form, this equation of state therefore doesn't make a similarly unrealistic assumption. This equation of state is obtained by determining the ionization fractions via two Saha equations. If n_n denotes the density of neutral helium, n_1 the density of He^+, and n_2 the density of He^{2+} then we have,

$$\frac{n_1 n_e}{n_n} = 4\left(\frac{2\pi m_e k_B T}{h^2}\right)^{3/2} e^{-\epsilon_1/k_B T} = K_1, \quad (6)$$

and,

$$\frac{n_2 n_e}{n_1} = \left(\frac{2\pi m_e k_B T}{h^2}\right)^{3/2} e^{-\epsilon_2/k_B T} = K_2, \quad (7)$$

where ϵ_1 and ϵ_2 are the first and second ionization energies respectively (24.6 and 54.4 eV). Introducing $n_0 = \rho/(4m_p)$, and the ionization fractions $f_1 = n_1/n_0$ and $f_2 = n_2/n_0$ we can cast this as two coupled equations,

$$f_1^2 + 2f_1 f_2 - (1-f_1-f_2)J_1 = 0, \quad (8)$$

and,

$$2f_2^2 + f_1 f_2 - J_2 f_1 = 0. \quad (9)$$

In the preceding two equations, $J_1 = K_1/n_0$ and $J_2 = K_2/n_0$. The equation of state is then defined by,

$$P = n_0 k_B T(1+f_1+2f_2), \quad (10)$$

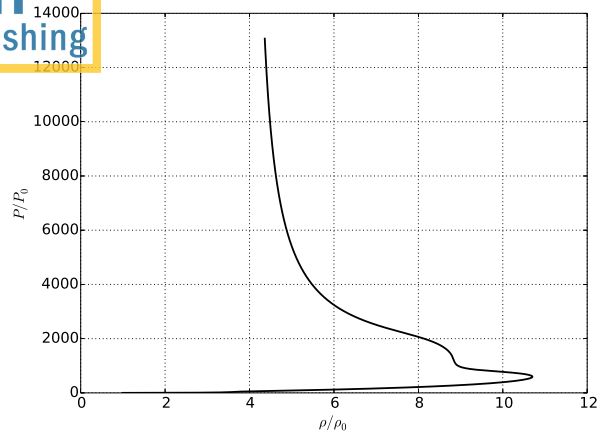

FIG. 2. Plot of Hugoniot curve calculated using the helium EOS model for ρ_0 =0.00668 kgm^{-3} and T_0 =0.1 eV.

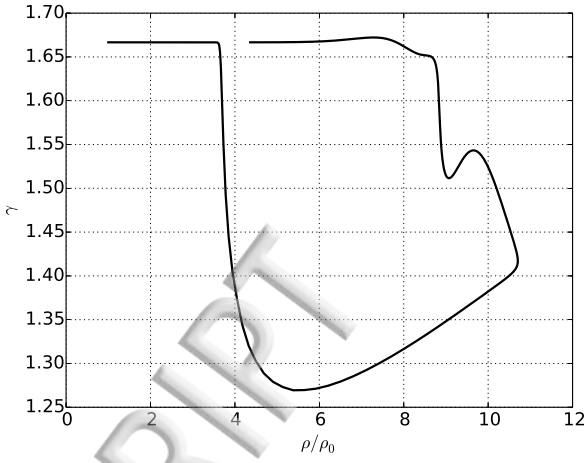

FIG. 3. Plot of ratio of specific heats for each of the post-shock states on the Hugoniot curve calculated using the helium EOS model for ρ_0 =0.00668 kgm^{-3} and T_0 =0.1 eV.

and,

$$U = \frac{3}{2} n_0 k_B T (1 + f_1 + 2f_2) + \epsilon_1 n_0 f_1 + \epsilon_2 n_0 f_2. \quad (11)$$

Since Eq.s 8 and 9 can be solved numerically by application of the bivariate Newton-Raphson method, we can always obtain this equation of state numerically. The ratio of specific heats can likewise be computed as part of this procedure. It is also possible to use this equation of state to compute the Hugoniot curve for dilute He by numerically solving,

$$e_1 - e_0 + \frac{1}{2}\left(\frac{1}{\rho_1} - \frac{1}{\rho_0}\right)(P_1 + P_0) = 0, \quad (12)$$

for ρ_1 given T_1 and the pre-shock condition (T_0, U_0, ρ_0, and P_0). Note that e denotes the specific internal energy, i.e. $e = U/\rho$. In fig.2 we plot the Hugoniot curve for dilute helium for the pre-shock conditions for ρ_0 =0.00668 kgm^{-3} and T_0 =0.1 eV.

Fig. 2 shows that there are a set of post-shock states with a pressure ratio of only several hundred where a compression ratio in excess of 10 is achieved. For states of higher pressure ratio the compression ratio decreases, tending towards four as expected. For a polytropic equation of state the maximum compression ratio is $\mu_{max} = 1+2/(\gamma-1)$, so fig. 2 suggests that there are a set of post-shock states where γ <1.3. This is confirmed when we compute the ratio of specific heats, which are plotted in fig. 3, where we find that there is a significant region where the ratio of specific heats is less than 1.3.

We can therefore conclude that it is possible to drive a shock through dilute He gas which will result in a post-shock state where the ratio of specific heats is less than 1.3. In which case we can further conclude that this means that it is possible that a blast wave can be driven in dilute He gas which is subject to the Vishniac instability.

IV. SHOCK PROPAGATION IN MOLECULAR HYDROGEN

Having shown the possibility of the Vishniac instability occurring in dilute He, we will now attempt the same for dilute diatomic hydrogen. For this a more complex model is required. Although the basis of this model should also be two coupled Saha equations (one for molecular dissocation and one for the ionization of hydrogen atoms), there is the particular issue of correctly evaluating the molecular partition function. In light of this we have opted to use the model developed by Quartapelle and Muzzio[22]. This includes a carefully evaluated treatment of the molecular partition function and also includes the excited states of neutral hydrogen. The full technical details of the model are reasonably complex, and we therefore direct the reader to the original description for these.

Using Quartapelle and Muzzio's model we have calculated the Hugoniot curve for H_2 with an initial density of ρ =0.0334 kgm^{-3} and an initial temperature of T_0 = 500K. The Hugoniot curve that we obtained is plotted in fig. 4. The ratio of specific heats for these post-shock states is shown in fig. 5, and in terms of the shock wave Mach number in fig. 6.

In fig. 5 it can be seen that there is a significant region where $\gamma < 1.3$, which is expected given that a number of high compression ratio post-shock states can be seen in fig. 4. At low pressure ratios the ratio of specific heats is close to 1.4, which is expected for a diatomic gas with five degrees of freedom. At high pressure ratios it can be seen that the ratio of specific heats tends towards 5/3, as expected once dissociation and ionization are complete. In terms of the shock wave's Mach number, fig. 6 shows that this occurs in the range $5 \leq M_s \leq 10$.

We therefore conclude that it is also the case that it is possible to drive a shock wave through dilute H_2 gas

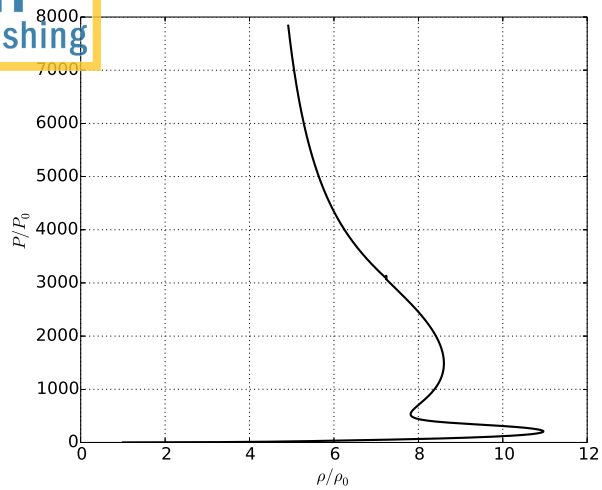

FIG. 4. Plot of Hugoniot curve calculated using Quartapelle and Muzzio's EOS model for H_2 with ρ_0 =0.0334 kgm^{-3} and T_0 = 500K.

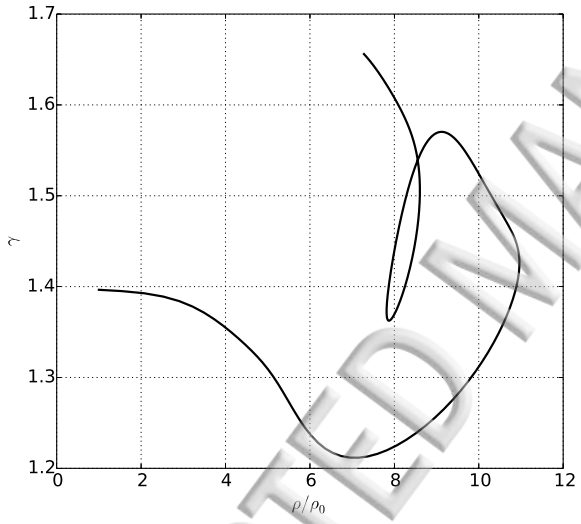

FIG. 5. Plot of ratio of specific heats for each of the post-shock states on the Hugoniot curve calculated using Quartapelle and Muzzio's EOS model for H_2 with ρ_0 =0.0334 kgm^{-3} and T_0 = 500K.

which results in a post-shock state where γ <1.3, and thus we can also conclude that a blast wave propagating in dilute H_2 gas can be subject to the Vishniac instability.

V. SIMULATIONS

A. Set-Up

We carried out numerical simulations using the ARCTURUS hydrodynamics simulation code. This code uses

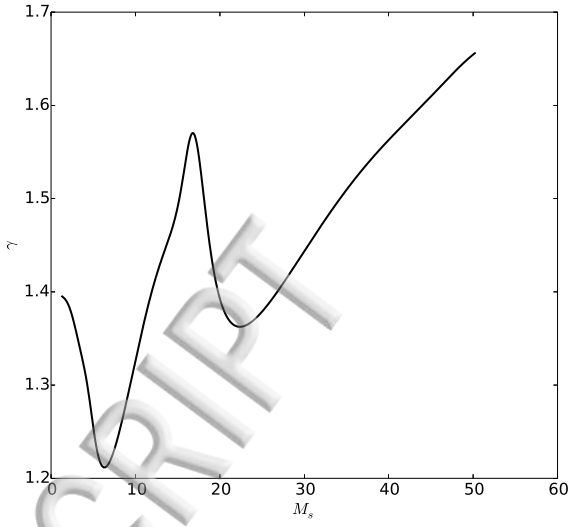

FIG. 6. Plot of ratio of specific heats for each of the post-shock states on the Hugoniot curve calculated using Quartapelle and Muzzio's EOS model for H_2 with ρ_0 =0.0334 kgm^{-3} and T_0 = 500K, in terms of the shock wave Mach number.

the method of Ziegler[23] to solve the equations of Eulerian hydrodynamics. There is no radiative cooling in this model. The version of the code employed in this study can also use tabulated equations of state. The simulations were initialized with the domain mainly consisting of an ambient medium at a density of ρ = 0.0334 kgm^{-3} and an internal energy density of U =6 $\times$ 10^{5}Jm^{-3}. A region centred around the mid-point in y and running along the entire length of the x-axis consisted of hot, dense fluid. The boundary of this region was defined by,

$$\mid y - y_m \mid < a\,(1 + \delta \cos{(kx)})\,, \qquad (13)$$

where y_m is the mid-point in y, a =50 μm, δ =0.05, and k =47124 m^{-1}. The density of this region was set to ρ_h =0.3 kgm^{-3}, and the internal energy density was set to U_h =3.9$\times$10^8 Jm^{-3}. The standard run used a tabulated EOS that was calculated using the model of Quartapelle and Muzzio[22] for H_2.

Simulations were carried out using a 3200 $\times$ 3200 grid, with cell sizes of $\Delta x = \Delta y$ =0.125μm. Simulations were run up to 5 ns.

B. Results

In the standard run we observe that the layer of shocked material between the shock front and the contact discontinuity develops a regular growing perturbation. In fig.7 we show a plot of the mass density in one quadrant of the simulation. The shocked material is present in fig.7 as a thin layer in the range 50 $\leq y \leq$ 65 μm where

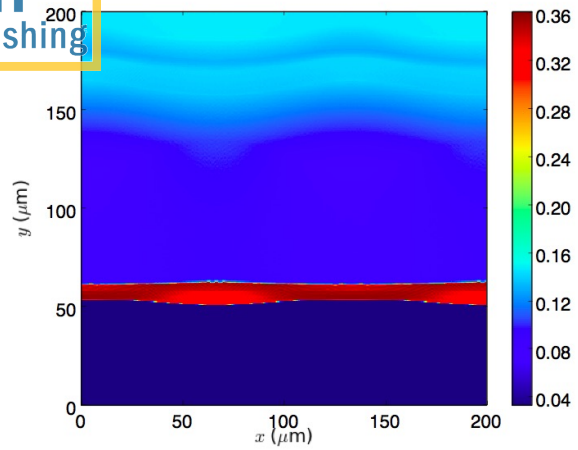

FIG. 7. Plot of mass density (kgm^{-3}) in one quadrant of the grid in the standard hydrodynamic simulation at 3.75 ns.

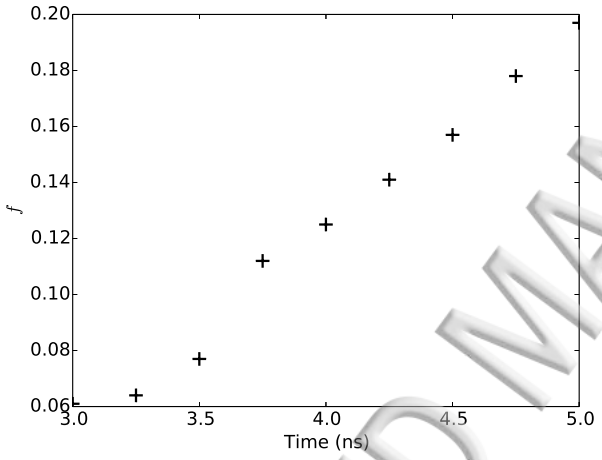

FIG. 8. Plot of f against time in the standard hydrodynamic simulation (see text).

ρ >0.3 kgm^{-3}. The perturbation running along the x-axis can also be seen, and it has a wavelength around 130μm which is close to the wavelength of the initial perturbation on the boundary of the hot region. Note that the compression ratio is in the range 9–10.

To quantify the development of this perturbation we determined the mid-point of the shocked layer at each time and then examined the line-outs of the mass density (along this mid-point in the x direction). We then calculated $f = (\rho_{hi} - \rho_{lo})/\rho_{lo}$ (where ρ_{hi} and ρ_{lo} are the crest and trough densities respectively). In fig. 8 we plot the results of this analysis.

This analysis is only possible after 3 ns as before this time the shocked layer is both too thin and too strongly corrugated for this analysis. When the standard run is repeated but with an ideal EOS instead of the H_2 (tabulated) EOS, then we find that there is no growing perturbation. We can therefore say that we have performed hydrodynamic simulations which show that a growing Vishniac-like instability appears. This occurs when we use an EOS that we have previously determined to be susceptible to the Vishniac instability, and when we choose initial conditions that create post-shock states that satisfy γ <1.3. Since the compression ratio is in the range 9–10, we know from fig. 5 that this is satisfied.

VI. CONCLUSIONS

The Vishniac instability is normally associated with strongly radiative blast waves, particularly SNRs in the later phases of their evolution. However, it has been noted that the Vishniac instability depends on the ratio of specific heats being sufficiently low, and does not rely on how this is achieved. This could be because the fluid has enough internal degrees of freedom, or it could be because there are routes through which energy can be lost. Ionization or dissociation processes can provide a route for energy loss. Here we have shown that $\gamma < 1.3$ can be achieved in three different models. These included both dilute He gas and dilute H_2 gas, where we further showed that $\gamma < 1.3$ occurs for certain post-shock states. This leads us to conclude that blast waves launched in these gases (and other types of shock waves) can be susceptible to the Vishniac instability. Furthermore we have presented the results of numerical simulations that support this conclusion.

We note that the threshold for the onset of the Vishniac instability (in terms of the ratio of specific heats) has been revised to γ ¡ 1.2 in other papers[8]. This applies to the case where the equation of state is polytropic, whereas the equations of state that we are interested in this paper are very different from any polytropic EOS. Given the inapplicability of previous theory, we have therefore employed numerical simulations to show the growth of a Vishniac-like mode. This paper therefore also raises the possibility that the true implications of the Vishniac instability may only be found by employing fully physical equations of state, and/or a fully physical treatment of radiative cooling — after all the low-γ polytropic EOS was only pursued as an model to facilitate study of the Vishniac instability.

There are two consequences of the conclusion we have reached. The first is that this should lead to a reconsideration of the interpretation of previous experiements, and a recognition that this complicates the interpretation of new experiments. A number of experiments have interpreted a rippling of the shock front, or other phenomena, as a manifestation of the D'yakov-Kontorovich instability, e.g. the corrugation seen at late times in the experiment reported by Nilson[20], however re-analysing these experiments in light of our results may lead to a different conclusion. The second consequence is that this opens up an unexplored route to studying the Vishniac instability (and related instabilities) in the laboratory.

The advantage of this approach is that it may avoid certain problems that have been encountered in the radiative flux regime, where it has been thought that radiation transport has reduced the compresssion ratio. The potential disadvantage is that $\gamma < 1.3$ is only achieved over a certain range of the shock wave's Mach number. This implies that when the shock wave speed is non-constant, that the shock front may only be susceptible to the Vishniac instability for a limited period.

Finally we note that, although the primary focus in this paper has been on the Vishniac instability, there are a number of other instabilities reported in the literature which depend on the post-shock fluid achieving γ close to 1. In particular there are the bow-shock instabilites described by Dgani *et al.*[11] and Ohnishi *et al.*[24], which, in light of the results reported in this paper, might be achieved due to ionization or dissociation.

Appendix A: Calculation of Ratio of Specific Heats

The expressions for internal energy and pressure can be converted into relations involving fluid volume, V, and total particle number, N. In this form one can use the familiar expressions for the heat capacity at constant volume,

$$C_v = \left(\frac{\partial U}{\partial T}\right)_V , \tag{A1}$$

and heat capacity at constant pressure,

$$C_p = C_v + T\left(\frac{\partial P}{\partial T}\right)_{V,N}\left(\frac{\partial V}{\partial T}\right)_{P,N} . \tag{A2}$$

Provided that we have expressions for U and P we can therefore evaluate γ analytically or numerically using these relations.

[1] J.W.Bates, Phys.Rev. E **91**, 013014 (2015).
[2] N.C.Freeman, Proc.R.Soc.London Ser. A **228**, 341 (1955).
[3] J.H.Gardner, D.L.Book, and I.B.Bernstein, J.Fluid Mech. **114**, 41 (1982).
[4] S.P.D'yakov, Zh.Eksp.Teor.Fiz. **27**, 288 (1954).
[5] J.W.Bates and D.C.Montgomery, Phys. Rev. Lett. **84**, 1180 (2000).
[6] K.Shigemori, T.Ditmire, B.A.Remington, V.Yanovsky, D.Ryutov, K.G.Estabrook, M.J.Edwards, A.J.MacKinnon, A.M.Rubenchik, and K.A.Keilty, Ap.J. **533**, L159 (2000).
[7] E.T.Vishniac, Ap.J. **274**, 152 (1983).
[8] D.Ryu and E.T.Vishniac, Ap.J. **313**, 820 (1987).
[9] E.T.Vishniac, Ap.J. **428**, 186 (1994).
[10] C.Michaut, C.Cavet, S.E.Bouquet, F.Roy, and H.C.Nguyen, Ap.J. **759**, 78 (2012).
[11] R.Dgani, D.V.Buren, and A.Noriega-Crespo, Ap.J. **461**, 927 (1996).
[12] G.Garcia-Segura and J.Franco, Ap.J. **469** (1996).
[13] N.Langer, G.Garcia-Segura, and M.-M. Low, Ap.J. **520**, L49 (1999).
[14] J.Grun, J.Stamper, C.Manka, J.Resnick, R.Burris, J.Crawford, and B.H.Ripin, Phys. Rev. Lett. **66**, 2738 (1991).
[15] M.J.Edwards, A.J.MacKinnon, J.Zweiback, K.Shigemori, D.Ryutov, A.M.Rubenchik, K.A.Keilty, E.Liang, B.A.Remington, and T.Ditmire, Phys. Rev. Lett. **87**, 085004 (2001).
[16] A.D.Edens, R.G.Adams, P.Rambo, L.Ruggles, I.C.Smith, J.L.Porter, and T.Ditmire, Phys. Plasmas **11**, 4968 (2004).
[17] D.R.Symes, M.Hohenberger, J.Lazarus, J.Osterhoff, A.S.Moore, R.R.Fäustlin, A.D.Edens, H.W.Doyle, R.E.Carley, A.Marocchino, J.P.Chittenden, A.C.Bernstein, E.T.Gumbrell, M.Dunne, R.A.Smith, and T.Ditmire, High Energy Density Phys. **6**, 274 (2010).
[18] R.P.Drake, F.W.Doss, R.G.McClarren, M.L.Adams, N.Amato, D.Bingham, C.C.Chou, C.DiStefano, K.Fidowski, B.Fryxell, T.I.Gombosi, M.J.Grosskopf, J.P.Holloway, B. der Hoist, C.M.Huntington, S.Kami, C.M.Krauland, C.C.Kuranz, and A.J.Visco, High Energy Density Phys. **7**, 130 (2011).
[19] N.J.Riley, S.M.Lewis, M.L.Wisher, M.W.Kimmel, K.W.Struve, J.L.Porter, R.D.Bengtson, and T.Ditmire, High Energy Density Phys. **22**, 64 (2017).
[20] P.M.Nilson, S.P.D.Mangles, L.Willingale, M.C.Kaluza, A.G.R.Thomas, M.Tatarakis, Z.Najmudin, R.J.Clarke, K.L.Lancaster, S.Karsch, J.Schreiber, R.G.Evans, A.E.Dangor, and K.Krushelnick, Phys.Rev.Lett. **103**, 255001 (2009).
[21] A.Lobel, L.Achmad, C. Jager, and H.Nieuwenhuijzen, Astron. Astrophys. **264**, 147 (1992).
[22] L.Quartapelle and A.Muzzio, Eur.Phys.J.D **69**, 156 (2015).
[23] U.Ziegler, J.Comput.Phys. **196**, 393 (2004).
[24] N.Ohnishi, Y.Sato, Y.Kikuchi, K.Ohtani, and K.Yasue, Phys.Fluids **27**, 066103 (2015).